Performance of a High Specific Impulse Hall Thruster

Bruce Pote and Rachel Tedrake
Busek Co. Inc.
11 Tech Circle
Natick, MA 01760-1023
busek@busek.com
508-655-5565

IEPC-01-35

Busek Co. Inc., in a SBIR program sponsored by the NASA Glenn Research Center, designed, and tested a nominally 1 kW thruster capable of both single stage and two-stage operation. This paper describes the results from detailed performance testing using several thruster geometries in both the single stage and two-stage configurations. Experimental testing revealed that specific impulses of greater than 3000 seconds at moderate applied voltage(s) (<1000 V) is feasible. Measured thrust, efficiency and Isp were obtained over a range of input power and propellant mass flowrates providing detailed characterization of both single and two-stage designs. In the single stage configuration, the measured thrust was 88 mN and 3000 sec Isp at an input power of 2.3 kW into the discharge. In the two-stage configuration, the maximum Isp obtained was 3300 seconds, also at 2.3 kW input power. The experimental results are used to compare and contrast the performance of single stage and two-stage operation. Data was comparable in both configurations and showed little advantage for this style of two stage operation. Also presented are the results from a simple analytical model that is used to characterize and understand the performance of the thruster(s). The model, applicable to all sizes and types of Hall thrusters, is useful in correlating the measured thrust and Isp expressed in terms of two global parameters, primary electron utilization and a lumped voltage loss. Analysis of the data using the model show that electron utilization efficiency is an important parameter for increasing thrust efficiency at high Isp.

Introduction

Hall thrusters were originally invented in the 1960's under the NASA research program in solar electric propulsion. Whether of the style under development at Busek, or the ceramic-lined long channel design known as the Stationary Plasma Thruster (SPT), or the metal wall, short channel type known as the Thruster with Anode Layer (TAL), they all use a single electrode pair consisting of an upstream anode located within the discharge chamber and an external cathode.

The alternative two-stage design actually proceeded in time the development of the single stage thruster[1,2]. In this configuration the Hall thruster contains an additional annular electrode biased at some intermediate potential between the upstream anode and that of the cathode. This style of two-stage thruster divides the discharge chamber into two zones with distinct functions, an ionization zone and an acceleration zone. Ionization occurs between the anode and the intermediate electrode due to the locally high number density of neutrals. Ion acceleration and some additional ionization occur in the downstream <z> direction at the exit plane of the thruster where the neutral number density is low, the radial magnetic field is high and where the electron number density is high due to incoming electrons being trapped on the magnetic flux lines. The potential advantage of the two-stage thruster is to de-couple and independently control the ionization process from the acceleration process.

Presented as Paper IEPC-01-35 at the 27th International Electric Propulsion Conference, Pasadena, CA, 15-19 October, 2001

To develop a Hall thruster propulsion system with a reduced wet mass, which is desirable in general, and essential for long duration solar system exploration as well as LEO to GEO transportation[3], the thruster must operate at high Isp typically exceeding 3000 seconds. At present, only gridded ion engines provide performance in the > 3000 second range and there is strong motivation to extend the operating envelope of state-of-the art Hall thrusters to fulfill such mission requirements[4,5].

Existing xenon fueled Hall thrusters typically operate in the 1500 – 2000 second Isp range, and the upper limit of operation has been gradually increased to 2500 seconds through incremental design improvements and by simply increasing the applied voltage. However, high-energy ion bombardment of the plasma wetted surfaces, and the inefficiency associated with multiple ionization as the applied voltage is increased raises questions about the validity of this approach in the 3500 second range.

To address the need for measurements on the performance characteristics of commercial Hall thrusters in the 3000 second specific impulse range, the Busek Co. designed, constructed and tested an nominal 1 kW thruster designated BHT-HD-1000 in a SBIR program sponsored by the NASA Glenn Research Center (GRC). The specific objective was to demonstrate 3000 second Isp at 2300 watts input power to the discharge while generating 100 mN of thrust.

This report summarizes the important test results from our laboratory model thruster. The performance of the engine was measured in both the conventional single-stage mode as well as a two-stage configuration.

Thruster Description

The desired operating point of the high Isp thruster involved a factor of two increase in Isp compared with typical designs developed and tested by Busek. AS a convenient means of scaling from other demonstrated designs, and to compare with previous experimental results, we used 300 V (discharge voltage) as the design point. For this reason the thruster is designated BHT-1000 a 1000 W input class thruster at 300 V.

The approach used to design the thruster relied heavily on our proven scaling techniques for single stage, nominal 300 V Hall thrusters in the 600 W to 8 kW power range. The basic criteria used at Busek and elsewhere[6] that can be derived and applied to the scaling of a Hall thruster is based on the fundamental relationship of the acceleration length (L) to the ion Lamor Radius (ρ_i) the electron Lamor radius (ρ_e) and ion - neutral mean free path (λ) defined as

$$L > \rho_e = \frac{m_e \upsilon_e}{qB} \quad L << \rho_i = \frac{m_i \upsilon_i}{qB} \quad L < \lambda \approx \frac{1}{n_n Q_{in}} \quad [1]$$

where n_n is the neural number density, υ is the velocity, m is the mass of the electrons and ions as denoted by the subscripts.

To maintain constants ρ_e, ρ_i, λ and υ

$$n_n \sim n_i = n_e \sim \frac{1}{L}$$

$$B \sim \frac{1}{L}$$

$$V_{dis} \sim \text{invariant} \Rightarrow \mathrm{E} \sim \frac{1}{\mathrm{L}}$$

$$I_{dis} = n_i \sigma_i q A \sim \left(\frac{1}{L}\right)(L)^2 \sim L$$

$$J_{dis} = I_{dis} / A \sim \frac{1}{L} \quad [2]$$

$$\text{Power} = V_{dis} I_{dis} \sim L$$

These equations relate the thruster characteristic dimension L to plasma parameters, which are then related to discharge geometric parameters such as mid-diameter of the discharge chamber, radial gap between the magnet poles and the radial gap of the discharge cavity, thus bridging the relationship of plasma parameters to thruster geometry. Magnet pole dimensions are determined using Gauss' and Ampere's law and pole piece insulator thickness are selected for lifetime requirements using a first order wall erosion/sputtering model.

The requirement for high Isp, and consequently higher discharge voltage required a higher B-field capability then nominally used for 300 V operation ($B \sim 1/L \sim V_{dis}$). This led us to deviate somewhat from the scaling laws of Eqs. [1, 2] and increase the mid diameter of the thruster from 62 mm to 68 mm. Increasing the mid cavity diameter also served to reduced the power density within the discharge chamber allowing an increase in the center pole diameter and more magnet coil turns while avoiding saturation of the magnetic circuit. We selected Hiperco 50 A alloy as the main magnetic material, which is an iron, cobalt, vanadium alloy, with a higher saturation field, permeability and Curie point than magnetic iron.

A photograph of the assembled thruster is shown in Figure 1. One of the key design features, that we incorporated specifically for high voltage operation was an integrally mounted high voltage propellant isolator. The isolator uses a high purity alumina barrel that contains a spiral propellant passage. The spiral design increases the effective length of the isolator and eliminates direct line of sight between the high and low voltage connections. Independent testing of the isolator showed threshold breakdown voltages of greater than 2500 V.

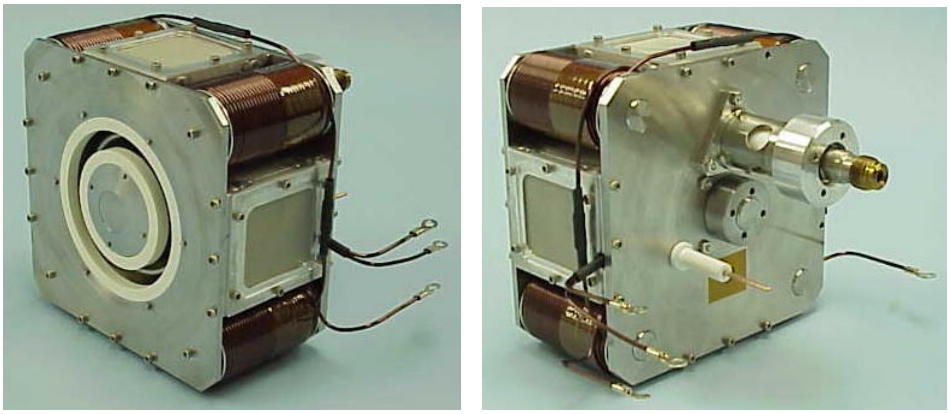

Figure 1 Photographs of the thruster designed and constructed for high Isp development

The key features of our patented[7] design are embodied in the configuration of the discharge chamber. It employs a combination of features that contribute to high performance and also facilitate two-stage operation. A schematic of the discharge chamber is illustrated in Figure 2. The major features are the composite anode, consisting of an inner, conically shaped wedge and an outer anode sometimes referred to as the outer anode housing. The inner anode also serves as the propellant distributor. Propellant enters the discharge chamber through a set of large radial holes such that the flow has initially zero axial momentum thus ensuring a long residence time. The radial holes are fed by a set of chocked orifice holes that are supplied by a common plenum. The outer housing has a relatively large volume that serves as a propellant reservoir for improved distribution and flow uniformity. This feature has been shown experimentally to reduce the magnitude of discharge current oscillations.

The inner anode and outer housing can also be designed to operate at different electrical potential, and serves as the basis for the initial segmented (two-stage) electrode approach. The outer anode housing can also be made of magnetic material to serve as a magnetic shunt for shaping the magnetic field profile and to establish the axial position of the plasma sheath. The primary effect of the shunt is to steepen the axial gradient of the radial B-field and to shift the maximum Br as far downstream (axially) as possible which translates into longer thruster life and importantly broadens the range of operating voltage.

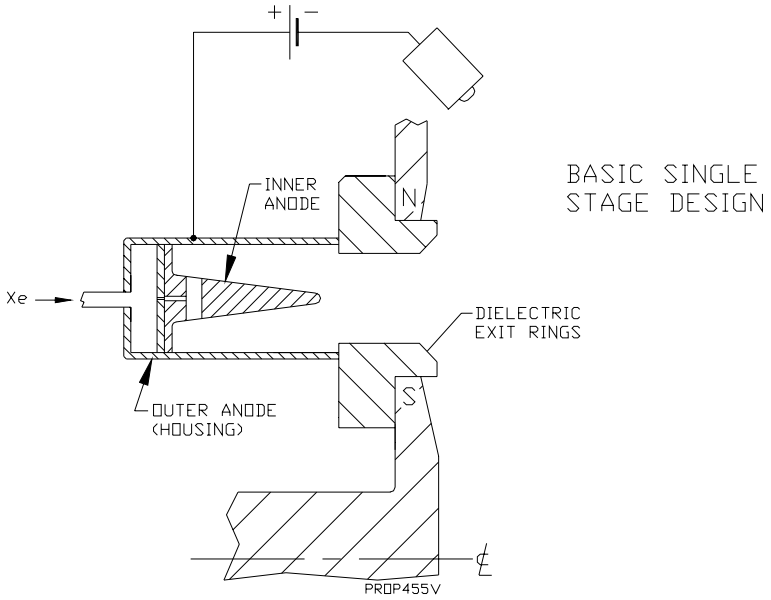

Figure 2 Basic single stage configuration of the BHT thruster illustrating the composite anode/discharge chamber arrangement.

Test Facilities and Instrumentation

Busek Co. maintains two of the largest privately owned, propulsion test facilities dedicated to testing of Hall effect thrusters. These cryogenic, high pumping speed facilities are essential for maintaining the high vacuum conditions necessary for accurate performance measurements. The facilities are equipped with in-situ diagnostics and performance measurement instrumentation that we use to optimize Hall thruster designs.

Mounted inside each tank is a thrust stand custom fabricated by Busek of the inverted pendulum style developed by NASA Glenn Research Center.[8] The thrust stand is water cooled, has in-situ calibration, and inclination control measured using a capacitive inclinometer. The output voltage from a linear variable differential transformer (LVDT), which is proportional to the thrust, is measured and recorded using the DAS and a strip chart recorder. The experimental procedure used to calibrate the thrust stand prior to and post experiment is similar to that described by Haag.[8]

For the testing conducted with the BHT-HD-1000, the T6 vacuum facility was used. This facility, shown in Figure 3 is comprised of two liquid nitrogen (LN_2) cooled sections, one where the experimental apparatus is located, the second where the cryogenic pumping is accomplished. The experimental section is 1.8 m in diameter and 2.4 m in length. The pumping section expands to 2.4 m in diameter and is 1.2 m long. The facility is roughed with a mechanical pump and blower. Vacuum pumping is accomplished with a combination of 0.8 m diameter diffusion pump and up to four single-stage cryopanels used to pump xenon. The total measured pumping speed is approximately 90,000 liters/second of xenon.

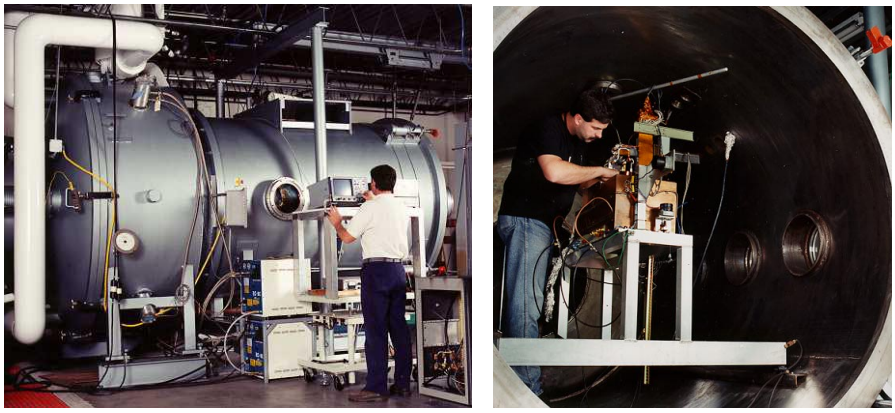

Figure 3 The T6 vacuum test facility at Busek

Data is recorded using a 12-bit, optically-isolated computerized DAS. The DAS measures and records discharge power, setting and recording the commercial mass flow controllers, recording the LVDT and inclination output of the thrust stand, vacuum tank pressure and anode and cathode internal pressure.

The propellant was supplied to the thruster and cathode through commercial mass flow controllers, calibrated for xenon. In addition, we also conduct periodic calibrations using an in-house designed flow calibration set-up that uses both constant pressure and constant volume techniques. These methods yield calibration curves that are within 5% of each other. Accuracy of the UNIT/MKS flowmeters is <2% according to the manufacturer. Tank pressure is measured using a Granville-Philips ion gauge calibrated for nitrogen. The propellant used was research grade xenon having a purity of 99.9995.

Testing was conducted to evaluate the performance of the thruster over a range of propellant mass flow rates and discharge voltages (up to 1000 volts) resulting in a range of input power from 200 W to 2.5 kW. The expellant flow rate to the commercial hollow cathode was maintained at 10% of the mass flow to the anode.

The electrical configuration for the single stage tests is shown in the schematic of Figure 4. For all tests the thruster body was grounded and the cathode allowed to float, typically below ground around 10-15 V. Commercially available power supplies were used to operate the discharge, cathode heater and keeper and all magnets. The facility pressure was, depending on the total flowrate, between 2-4x10^{-6} torr. No correction for the effects of facility background xenon pressure are therefore required in the data presented.

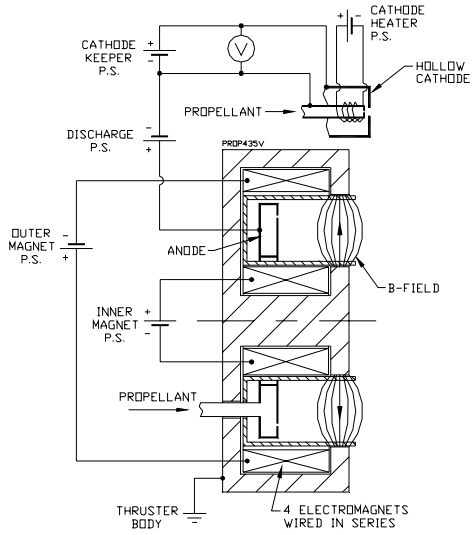

Figure 4 Electrical schematic for single stage testing of the BHT-1000

The test procedure followed an established pattern for testing Hall thrusters used by Busek and others[9]. The cathode was heated and started using its keeper, the thruster mass flow was established using the mass flow controller and the main discharge voltage was gradually applied to the thruster using a commercial power supply. The discharge power supply was operated in the voltage control mode. There was no external capacitor added as a filter to the discharge circuit. The discharge started at a typical voltage in the range of 50 to 60 Volts. The

thruster operated in a stable manner with no abnormal oscillations as measured by commercial RMS meters of both the discharge voltage and discharge current. At each operating point we attempted to adjust the inner and outer magnet currents to minimize the discharge current.

Major Test Results

The BHT-1000 thruster was operated in both a single stage and two-stage configuration over a range of propellant mass flow rates and discharge voltages. This resulted in a range of input power from 200 W to 2.5 kW. The single stage data is initially presented followed by our two-stage data.

Single Stage Testing

In the single stage configuration the thruster was tested with either a non-magnetic (stainless steel) outer housing or a magnetic (magnet iron ASTM A-848) outer housing. In this latter configuration, the outer housing acts as a magnetic shunt to shape the B-field profiles such that minimal ions impact the dielectric walls and are not wasted from a thrust standpoint while minimizing sputtering of the discharge chamber exit rings. Thruster performance was significantly improved with the magnetic housing and this data is further presented below. Performance of the thruster in the single stage mode was very encouraging although we did not achieve the desired goals of thrust and Isp at 2.3 kW simultaneously.

The data collected in the single stage configuration is summarized in Table 1. The V-I characteristics in the single stage configuration mode for three anode massflow rates are shown in Figure 5. Over the range of voltages tested the thruster had measured V-I characteristics typical of Hall thrusters. At low voltage the thruster operates as a resistive load with increasing discharge current with increasing voltage. This is followed by the characteristic transition to a negative impedance that corresponds to a visual change in the downstream plasma structure. We call this transition from the diffuse mode the jet mode. Above about 200 V the thruster discharge becomes very stable and begins to operate in a high efficiency mode where current becomes largely independent of the applied voltage. In the single stage configuration, at a discharge voltage of 450-500 V, the thruster undergoes another transition to a slightly positive slope until about 600-650 volts. At this voltage the current becomes largely independent of the voltage. The onset of this second transition also corresponds with a peak in thrust efficiency. Between 400 and 900 volts we did not observe any noticeable (visual) change in the downstream plasma. A photograph of the thruster firing inside the vacuum test chamber in Figure 6 shows clearly the highly luminus jet on the center axis of the thruster.

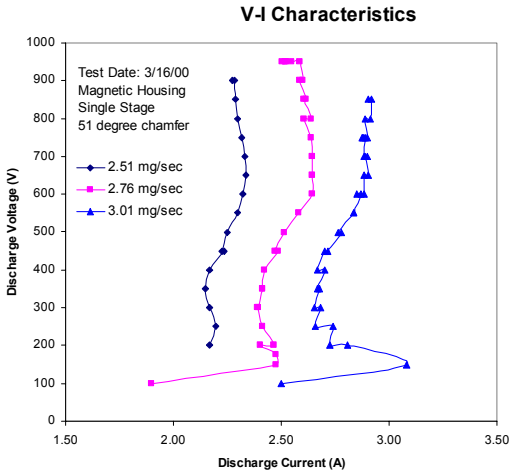

Figure 5 V-I characteristics in the single stage mode.

Table 1 Single Stage performance Results with the Magnetic Anode Housing

Thruster Flow Rate (mg/sec)	Cathode Flow Rate (mg/sec)	Total Flow Rate (mg/sec)	Discharge Current (A)	Acceleration Potential (V)	Discharge Power (W)	Thrust (mN)	A.Specific Impulse (sec)	Anode Efficiency (%)	Specific Thrust [mN/kW]
2.51	0.25	2.76	2.17	200	434.00	29.19	1185.58	39.12	67.26
2.51	0.25	2.76	2.20	250	548.75	35.60	1445.83	46.01	64.88
2.51	0.25	2.76	2.17	300	651.00	40.58	1648.25	50.40	62.34
2.51	0.25	2.76	2.15	350	752.50	44.86	1821.75	53.27	59.61
2.51	0.25	2.76	2.17	400	868.00	48.42	1966.33	53.80	55.78
2.51	0.25	2.76	2.24	450	1005.75	51.98	2110.91	53.51	51.68
2.51	0.25	2.76	2.23	450	1001.25	55.54	2255.49	61.37	55.47
2.51	0.25	2.76	2.25	500	1125.00	58.39	2371.16	60.36	51.90
2.51	0.25	2.76	2.30	550	1265.00	61.23	2486.83	59.04	48.41
2.51	0.25	2.76	2.32	600	1392.00	63.37	2573.58	57.47	45.52
2.51	0.25	2.76	2.34	650	1517.75	66.22	2689.24	57.55	43.63
2.51	0.25	2.76	2.33	700	1631.00	68.35	2775.99	57.06	41.91
2.51	0.25	2.76	2.32	750	1736.25	70.49	2862.74	57.01	40.60
2.51	0.25	2.76	2.30	800	1840.00	72.63	2949.49	57.10	39.47
2.51	0.25	2.76	2.29	850	1946.50	74.05	3007.33	56.12	38.04
2.51	0.25	2.76	2.29	900	2056.50	74.76	3036.24	54.14	36.35
2.51	0.25	2.76	2.28	900	2047.50	75.47	3065.01	55.41	36.86
2.76	0.27	3.03	1.90	100	190.00	14.24	525.95	19.34	74.95
2.76	0.27	3.03	2.48	150	371.25	24.21	894.11	28.60	65.21
2.76	0.27	3.03	2.48	175	433.13	28.48	1051.89	33.93	65.76
2.76	0.27	3.03	2.41	200	481.00	35.60	1314.87	47.73	74.01
2.76	0.27	3.03	2.47	200	493.00	26.34	973.00	25.50	53.44
2.76	0.27	3.03	2.42	250	603.75	41.30	1525.25	51.17	68.40
2.76	0.27	3.03	2.39	300	717.00	46.28	1709.33	54.12	64.55
2.76	0.27	3.03	2.40	300	718.50	45.57	1683.03	52.36	63.42
2.76	0.27	3.03	2.42	350	845.25	50.55	1867.11	54.77	59.81
2.76	0.27	3.03	2.42	350	845.25	49.84	1840.81	53.24	58.97
2.76	0.27	3.03	2.43	400	970.00	55.54	2051.19	57.60	57.25
2.76	0.27	3.03	2.49	450	1118.25	59.81	2208.98	57.95	53.48
2.76	0.27	3.03	2.47	450	1111.50	59.10	2182.68	56.92	53.17
2.76	0.27	3.03	2.52	500	1257.50	62.66	2314.17	56.56	49.83
2.76	0.27	3.03	2.58	550	1419.00	66.22	2445.65	55.98	46.66
2.76	0.27	3.03	2.65	600	1587.00	69.07	2550.84	54.45	43.52
2.76	0.27	3.03	2.65	650	1719.25	71.91	2656.03	54.49	41.83
2.76	0.27	3.03	2.65	700	1851.50	74.76	2761.22	54.69	40.38
2.76	0.27	3.03	2.64	750	1980.00	76.90	2840.11	54.10	38.84
2.76	0.27	3.03	2.61	800	2084.00	79.75	2945.30	55.28	38.27
2.76	0.27	3.03	2.64	800	2112.00	79.03	2919.00	53.58	37.42
2.76	0.27	3.03	2.61	850	2214.25	81.17	2997.90	53.90	36.66
2.76	0.27	3.03	2.62	850	2222.75	81.17	2997.90	53.70	36.52
2.76	0.27	3.03	2.59	900	2326.50	84.02	3103.09	54.97	36.11
2.76	0.27	3.03	2.60	900	2340.00	83.31	3076.79	53.73	35.60
2.76	0.27	3.03	2.59	950	2455.75	85.44	3155.68	53.85	34.79
2.76	0.27	3.03	2.55	950	2422.50	86.15	3181.98	55.51	35.56
2.76	0.27	3.03	2.53	950	2398.75	86.87	3208.27	56.99	36.21
2.76	0.27	3.03	2.52	950	2394.00	86.15	3181.98	56.17	35.99
2.76	0.27	3.03	2.52	950	2394.00	86.15	3181.98	56.17	35.99
2.76	0.27	3.03	2.51	950	2379.75	85.44	3155.68	55.57	35.90
3.01	0.30	3.31	2.50	100	250.00	24.01	813.29	38.32	96.06
3.01	0.30	3.31	3.08	150	462.00	30.37	1028.57	33.17	65.74
3.01	0.30	3.31	2.81	200	562.00	38.14	1291.69	43.00	67.87
3.01	0.30	3.31	2.73	200	545.00	38.14	1291.69	44.34	69.98
3.01	0.30	3.31	2.74	250	685.00	44.50	1506.98	48.02	64.96
3.01	0.30	3.31	2.66	250	665.00	45.20	1530.90	51.04	67.98
3.01	0.30	3.31	2.69	300	805.50	50.86	1722.26	53.33	63.13
3.01	0.30	3.31	2.66	300	796.50	50.15	1698.34	52.45	62.96
3.01	0.30	3.31	2.68	350	938.00	55.09	1865.78	53.75	58.73
3.01	0.30	3.31	2.67	350	934.50	55.09	1865.78	53.95	58.95
3.01	0.30	3.31	2.70	400	1080.00	59.33	2009.30	54.14	54.94
3.01	0.30	3.31	2.67	400	1068.00	60.04	2033.22	56.06	56.21
3.01	0.30	3.31	2.70	450	1215.00	66.39	2248.50	60.27	54.65
3.01	0.30	3.31	2.72	450	1221.75	65.69	2224.58	58.67	53.77
3.01	0.30	3.31	2.78	500	1390.00	68.51	2320.27	56.10	49.29
3.01	0.30	3.31	2.77	500	1382.50	69.22	2344.19	57.57	50.07
3.01	0.30	3.31	2.84	550	1559.25	72.75	2463.79	56.39	46.66
3.01	0.30	3.31	2.84	550	1559.25	72.04	2439.87	55.30	46.20
3.01	0.30	3.31	2.87	600	1722.00	74.87	2535.55	54.07	43.48
3.01	0.30	3.31	2.85	600	1710.00	75.58	2559.47	55.49	44.20
3.01	0.30	3.31	2.89	600	1731.00	76.28	2583.39	55.84	44.07
3.01	0.30	3.31	2.89	650	1875.25	78.40	2655.15	54.45	41.81

Figure 6 Photographs of the thruster firing showing the characteristic jet on the center axis of the discharge plume

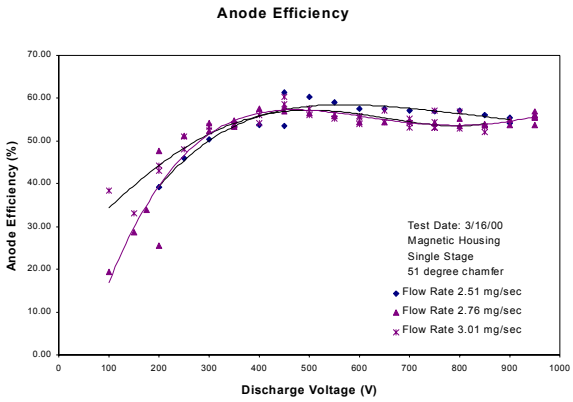

Figure 7 Efficiency versus discharge voltage in the single stage mode

The thruster performance, in terms of thrust efficiency versus voltage is plotted in Figure 7. The plot shows a peak in the calculated efficiency at 450-500 volts that corresponds to the second transition to a positive slope in the V-I curve of Figure 6. Possible explanations for the increase in discharge current with applied voltage and peak in thrust efficiency can be attributed to an increase in the fraction of doubly charged xenon ions or due to increased electron current as will be discussed in more detail later in the paper.

Two-stage Testing

Two-stage testing was also conducted in our T6 test chamber as described in the previous subsection. An additional isolated power supply is used to power the first stage ionization zone, independently from the second stage acceleration zone. The electrical configuration for two stage testing is shown in Figure 8. The electrical schematic also illustrates qualitatively the two-stage concept where the first stage operates primarily as an ionization zone and the exit region acts primarily as the ion accelerator.

Tests were conducted with both the non-magnetic and magnetic outer anode housing. To facilitate two-stage testing, the discharge chamber shown in Figure 2 was modified to provide electrical isolation between the inner anode (wedge) and the outer discharge chamber housing. The geometry of the anode arrangement is nearly identical to the test configuration evaluated during single stage testing. Only the data obtained with the magnetic housing is reported.

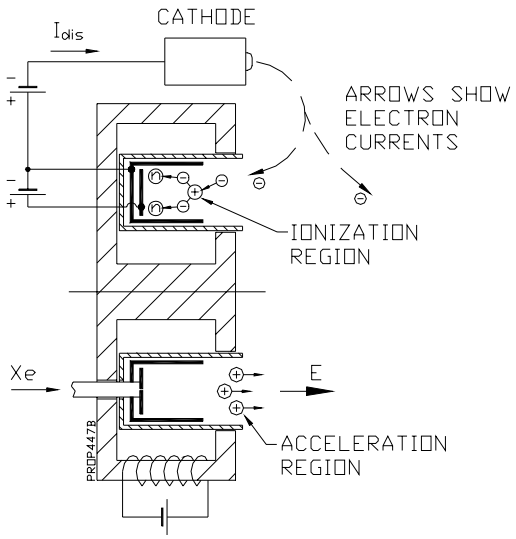

Figure 8 Electrical schematic for two-stage testing

In Table 2 the data obtained with the magnetic housing is summarized. In this configuration the maximum anode specific impulse obtained was over 3300 seconds corresponding to a total voltage of 1000 volts. The ionization voltage was varied from 50 - 150 volts with little affect on thruster performance. This represents about 200 seconds Isp increase over the maximum obtained in the single stage mode. Similar to the single stage performance the thruster operation was limited by overheating of the inner magnetic pole and inner pole insulator. We suspect that overheating causes a reduction in magnetic flux capacity through the inner pole and a loss of dielectric properties along the surface of the insulator. Both result in current leakage to the thruster causing the discharge to extinguish.

A typical measured V-I characteristic for the thruster in the two-stage mode is plotted in Figure 9. Here we plot just the acceleration voltage versus the discharge current for an anode mass flowrate of 2.00 mg/sec. We see very little influence of the ionization voltage on the V-I in the acceleration stage. We also see very similar V-1 characteristics comparing single stage and two-stage performance.

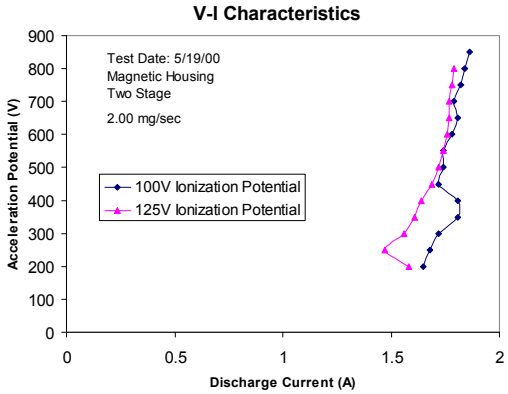

Figure 9 V-I characteristic of the acceleration stage in the two-stage mode. The first stage ionization voltage has little effect on resulting second stage V-I

Table 2 Two-Stage Performance with the Non-Magnetic Outer Housing

Thruster Flow Rate (mg/sec)	Cathode Flow Rate (mg/sec)	Total Flow Rate (mg/sec)	Ionization Current (A)	Ionization Potential (V)	Discharge Current (A)	Acceleration Potential (V)	Discharge Power (W)	Thrust (mN)	A.Specific Impulse (sec)	Anode Efficiency (%)	Specific Thrust [mN/kW]
1.38	0.14	1.52	1.37	50.00	1.32	129	238.78	15.77	1164.60	37.72	66.03
1.38	0.14	1.52	1.35	50.00	1.31	200	329.50	17.87	1319.88	35.11	54.23
1.38	0.14	1.52	1.46	50.00	1.43	250	430.50	21.02	1552.80	37.19	48.83
1.38	0.14	1.52	1.22	30.00	1.39	300	453.60	22.07	1630.43	38.92	48.66
1.38	0.14	1.52	1.48	100.00	1.41	400	712.00	32.58	2406.83	54.03	45.76
1.38	0.14	1.52	1.60	100.00	1.52	400	768.00	26.28	1940.99	32.57	34.21
1.38	0.14	1.52	1.55	100.00	1.48	400	747.00	26.28	1940.99	33.49	35.18
1.38	0.14	1.52	1.51	125.00	1.43	400	760.75	34.69	2562.11	57.30	45.59
1.38	0.14	1.52	1.48	125.00	1.40	400	745.00	34.16	2523.29	56.75	45.85
1.38	0.14	1.52			1.49	450	670.50	24.17	1785.71	31.58	36.05
1.38	0.14	1.52	1.36	125.00	1.28	500	810.00	33.63	2484.47	50.60	41.52
1.38	0.14	1.52	1.37	125.00	1.34	600	975.25	37.84	2795.03	53.19	38.80
1.63	0.16	1.79	1.25	100.00	1.15	200	355.00	21.02	1314.64	38.18	59.22
1.63	0.16	1.79	1.26	100.00	1.20	300	486.00	23.12	1446.10	33.75	47.58
1.63	0.16	1.79	1.38	100.00	1.32	400	666.00	27.33	1709.03	34.40	41.03
1.63	0.16	1.79	1.54	100.00	1.48	500	894.00	33.63	2103.42	38.82	37.62
1.63	0.16	1.79	1.51	100.00	1.48	600	1039.00	37.84	2366.35	42.27	36.42
1.63	0.16	1.79	1.56	100.00	1.54	700	1234.00	39.42	2464.94	38.62	31.94
2.00	0.20	2.20	1.57	150.00	1.43	100	378.50	25.23	1285.71	42.03	66.65
2.00	0.20	2.20	1.69	150.00	1.50	200	553.50	31.53	1607.14	44.91	56.97
2.00	0.20	2.20	1.74	100.00	1.57	300	645.00	34.69	1767.86	46.63	53.78
2.00	0.20	2.20	1.76	150.00	1.56	300	732.00	36.79	1875.00	46.22	50.26
2.00	0.20	2.20	1.76	100.00	1.61	400	820.00	40.47	2062.50	49.92	49.35
2.00	0.20	2.20	1.76	150.00	1.60	400	904.00	41.52	2116.07	47.67	45.93
2.00	0.20	2.20	1.70	100.00	1.65	500	995.00	44.67	2276.79	50.14	44.90
2.00	0.20	2.20	1.56	100.00	1.68	600	1164.00	47.30	2410.71	48.05	40.63
2.00	0.20	2.20	1.76	150.00	1.68	600	1272.00	48.87	2491.07	46.95	38.42
2.00	0.20	2.20	1.55	100.00	1.72	700	1359.00	50.45	2571.43	46.82	37.12
2.50	0.25	2.75	2.07	100.00	1.97	100	404.00	28.90	1178.57	41.36	71.55
2.50	0.25	2.75	2.15	150.00	1.93	100	515.50	33.63	1371.43	43.89	65.25
2.50	0.25	2.75	2.18	100.00	1.97	200	612.00	38.89	1585.71	49.42	63.55
2.50	0.25	2.75	2.28	150.00	2.04	200	750.00	42.04	1714.29	47.14	56.06
2.50	0.25	2.75	2.23	100.00	2.02	300	829.00	46.77	1907.14	52.78	56.42
2.50	0.25	2.75	2.22	150.00	2.00	300	933.00	49.40	2014.29	52.31	52.95
2.50	0.25	2.75	2.22	100.00	2.04	400	1038.00	52.55	2142.86	53.22	50.63
2.50	0.25	2.75	2.27	150.00	2.05	400	1160.50	56.23	2292.86	54.50	48.46
2.50	0.25	2.75	2.20	100.00	2.09	500	1265.00	59.91	2442.86	56.75	47.36
2.50	0.25	2.75	2.33	150.00	2.13	500	1414.50	62.01	2528.57	54.37	43.84
2.50	0.25	2.75	2.16	100.00	2.14	600	1500.00	64.64	2635.71	55.71	43.09
2.50	0.25	2.75	2.38	150.00	2.20	600	1677.00	65.17	2657.14	50.65	38.86
2.50	0.25	2.75	2.40	150.00	2.29	700	1963.00	71.47	2914.29	52.05	36.41
2.50	0.25	2.75	2.48	175.00	2.31	700	2051.00	73.58	3000.00	52.79	35.87

Plotted in Figure 10 is the anode thrust efficiency as a function of the acceleration voltage (~Isp^2). We see some of the same general trends that appear from the single stage testing. The thrust efficiency reaches a maximum at a voltage of 500-600 volts some 100 to 150 volts higher than the corresponding single stage case. In addition there is very little effect of first stage ionization voltage on the efficiency. We also note that there is very little difference in thrust efficiency between single stage and the two-stage mode of operation.

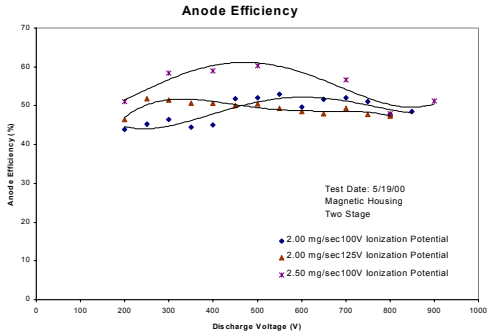

Figure 10 Efficiency versus acceleration voltage in the two-stage configuration

Comparison of Single Stage and Two-Stage Performance

To facilitate a direct comparison of single stage and two-stage performance, the data provided in Tables 1 and 2 is plotted as anode efficiency versus anode Isp in Figure 11. The experimental data shows that we generally reach an asymptote in thrust efficiency (regardless of the operating mode) at an Isp of 2500 seconds. The similar performance appears not to support the qualitative benefits of de-coupling the ionization and acceleration functions. Possible explanations for this behavior are discussed in the paper by Jacobsen et al[10]. The results obtained from during our testing provided similar conclusions.

In order to understand the physical phenomena of the thruster performance at high Isp we used a simple performance model developed at Busek[11] and described in some detail in Ref. 11. The model relies on two easily understandable parameters. One is the flux of cathode electrons that enter the thruster (*Iee*) to ionize the propellant normalized by the total discharge current (*Idis*). The other parameter is the energy or voltage losses (ΔV) during the ionization and acceleration process. This is comprised of all the voltage drops that contribute to the acceleration of the ions. Thus, the portion of the discharge voltage actually accelerating the ions can be written as

$$Vacc = Vdis - \Delta V \qquad [3]$$

while the magnitude of *Iee* is dictated by how many primary cathode electrons are needed to produce the total discharge current.

From this, we can express the thrust (T), the Isp and the efficiency (n) in terms of discharge power and the two loss parameters, i ($i = Iee/Idis$), and ΔV.

$$T = \dot{m}_t < u > \cong \dot{m}_i u_i \cong \left(\frac{2P_{dis}}{I_{sp}}\right)\frac{k_1(1-2i)}{1+\left(\frac{k_1\Delta u_i}{I_{sp}}\right)^2} \qquad [4]$$

$$I_{sp} = \frac{T}{\dot{m}_t g_o} \cong \frac{\dot{m}_i u_i}{\dot{m}_t g_o} \cong k_1(1-i)\sqrt{\frac{2q(V_{dis}-\Delta V_{ttl})}{m_i}} \qquad [5]$$

$$\eta = \frac{\frac{1}{2}\dot{m}_i u_i^2}{P_{dis}} \cong (1-i)\left(1-\frac{\Delta V_{ttl}}{V_{dis}}\right) \cong \frac{1-i}{1+\left(\frac{k_1\Delta u_i}{I_{sp}}\right)^2} \qquad [6]$$

where $k_1 = \left(\frac{I_{dis}}{\dot{m}_t g_o}\right)\left(\frac{m_i}{q}\right) \cong$ constant $\approx$ 0.139 for Xe,

$\Delta u_i = \sqrt{\frac{2q\Delta V_{ttl}}{m_i}} =$ ion velocity deficit due to ΔV_{ttl} loss

From the equation for efficiency (Eq. [6]), for a given i and ΔV the efficiency continuously increases with increasing voltage approaching an asymptotic value at about 4500 sec Isp. This is because the total voltage drop becomes less important when the ratio

of $\Delta V/Vdis$ becomes much less than one (i.e. at high applied voltage), and the efficiency becomes primarily a function of the electron loss parameter $n \approx (1\text{-}i)$.

Superimposed on the data in Figure 11 we plot model results following a trend of constant i and ΔV, the other with increasing electron loss parameter with increasing voltage above 2500 seconds Isp.

In our experimental data, we reached a peak in thrust efficiency at an Isp of around 2500 seconds. At constant electron loss and voltage drop this is substantially below that predicted by our model.

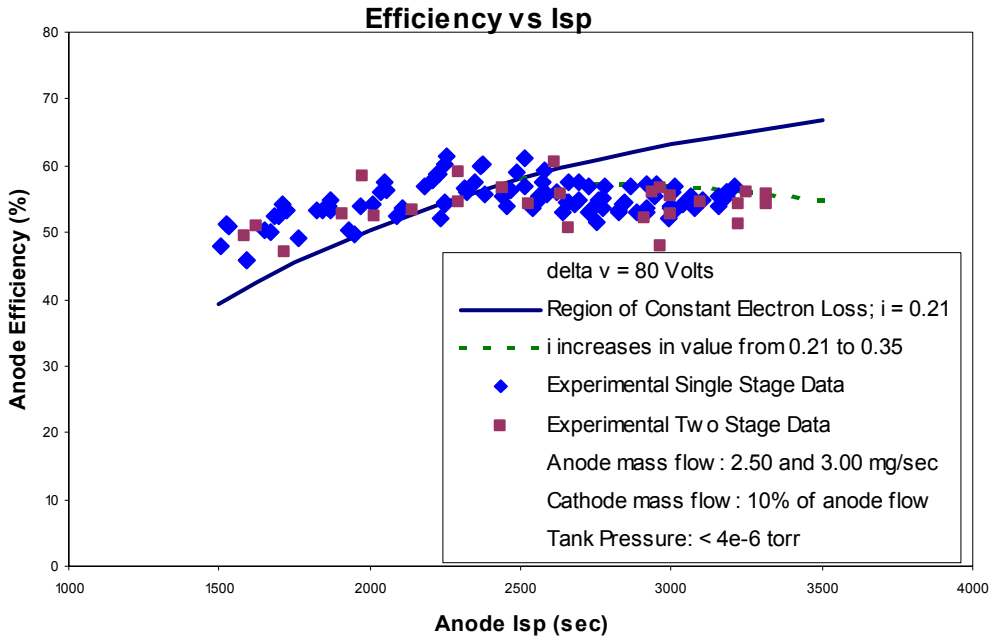

Figure 11 Comparison of single stage and two-stage data with our two parameter model. Up to 2500 sec follows a trend of constant i and ΔV. Above 2500 sec the electron loss parameter is increasing

Increasing electron loss with increasing discharge voltage as predicted by the model is one way to explain the observed data trend. The data could also be explained through an increase in ion current which would require a significant increase in the number of doubly/triply charged ions. Measurements at Busek and others[12] show there is a measurable fraction of doubly charged ions even at 300 V discharge voltage and their fraction do not significantly increase as the voltage is increased. Therefore we believe the phenomena is dominated by increased electron current transport across the magnetic field at higher voltages. Further testing will be performed to more definitively address this question and to understand fundamentally what drives the electron loss.

Conclusions

The BHT-1000 thruster was operated in both the single stage and two-stage configurations. In the single stage mode, at 2.3 kW input power we achieved a maximum of 88 mN at 3000 sec Isp corresponding to an anode propulsive efficiency of 57%. In the two-stage configuration we were able to operate the thruster at 3300 seconds Isp corresponding to a total applied voltage of 1000V. In the two-stage configuration the thruster was operated with two power supplies in series biasing an intermediate electrode at a voltage between the cathode and the upstream anode.

While the very aggressive performance goals of 100 mN and 3000 sec Isp at 2.3 kW were not match exactly the feasibility of operating our thruster in the 3000 sec Isp range at high efficiency was demonstrated. Thermal limitations, particularly overheating of the center stem and insulator surfaces limited the maximum input voltage to 1000 volts over the range of anode mass flow rates tested suggesting a slightly larger thruster may better optimized for the target operating requirements. There was no appreciable difference between the measured single stage and two-stage performance.

Our two parameter model, developed to predict Hall thruster performance given two global loss parameters (voltage and electron loss) has given insight into the fundamental mechanisms that control idealized thrust, efficiency and Isp behavior. Generally the efficiency reached an peak at 500 volts (+/-) corresponding to 2500 seconds Isp. This suggests a loss mechanism at discharge voltages greater than 500 volts which we believe to be caused by increasing electron loss, the efficiency by which the primary cathode electrons are used to ionize the propellant. Understanding the relationship of electron loss and high voltage operation is important for high Isp Hall thruster operation.

Acknowledgement

This work was performed under a Phase I Small Business Innovation Research Contract sponsored by NASA Glenn Research Center. The authors would like to thank the technical staff of the on-board propulsion group, in particular, Mr. R. Jankovsky and Mr. D. Jacobson for their ongoing support for high Isp thruster development at Busek.

1 Grishin, S.D., Erofeev, V.S., Zharinov, A.V., Naumkin, V.P. and Safronov, I.N., "Characteristics of a Two-Stage Ion Accelerator with an Anode Layer," Zhounal Prikladnoi Mkhaniki, I Tekhnicheskoi Fiziki, No. 2, pp 28-36, March-April 1978.

2 Tverdokhlebov, S., "Study of Double-Stage Anode Layer Thruster using Inert Gases," Paper IEPC-93-232, 23rd International Electric Populsion Conference, Seattle, WA, Sept. 1993.

3 Manzella, David H., Jacobson, David T., and Jankovsky, Robert S., "High Voltage SPT Performance," 37th AIAA Joint Propulsion Conference, Salt Lake City, UT, July 2001.

4 Muller, J., "Thruster Options for Microspacecraft: A Review and Evaluation of Existing Hardware and Emerging Technologies," Paper AIAA 97-3058, 33rd Joint Propulsion Conference, Seattle, July 1997.

5 Gluczinski, F.S. and Spores, R.A., "Analysis of Hall-Effect Thrusters and Ion Engines for Orbit Transfer Missions," AIAA paper 96-2673, July 1996.

6. Khayms, V. and Martinez-Sanchez, M., "Design of a Miniaturized Hall Thruster for Microsatellites, 32nd AIAA/ASME/SAE/ASEE Joint Propulsion Conference, Lake Buena Vista, FL, July 1996.

7 Busek Co. Inc. United States Patent No. 6,075,321, "Hall Field Plasma Accelerator with Inner and Outer Anode, Dated June 13, 2000.

8. Haag, T.M. and Osborn, M., "RHETT/EPDM Performance Characterization," IEPC-97-107, 25th IEPC, Cleveland, OH, August 1997.

9 Gavryushin, V., et al., "Study of the Effect of Magnetic Field Variations, Channel Geometry and its Wall Contamination Upon the SPT Performance," AIAA-94-2854, June 1994.

10 Jacobson, David T., Jankovsky, Robert S., Rawlin, Vincent K., and Manzella, David H., "High Voltage TAL Performance," 37th AIAA Joint Propulsion Conference, Salt Lake City, UT, July 2001.

11 Pote, B., Hruby, V., and Monheiser, J., "Performance of an 8 kW Hall Thruster," IEPC-99-080, 26th International Electric propulsion Conference, Kitakyushu, Japan, October 1999.

12 Personal Communication, Dr. A. Galimore, June 2000.